

A model-free continuous integral sliding mode controller for robust control of robotic manipulators

Günyaz Ablay

Department of Electrical-Electronics Engineering, Abdullah Gül University, Kayseri, Türkiye

Article Info

Article history:

Received Aug 12, 2022

Revised Sep 20, 2022

Accepted Oct 3, 2022

Keywords:

Model-free control

Robot control

Robotic manipulators

Robust control

Sliding mode control

ABSTRACT

This paper proposes a model-free continuous integral sliding mode controller for robust control of robotic manipulators. The highly nonlinear dynamics of robots and load disturbances cause control challenges. To achieve tracking control under load disturbances and nonlinear parameter variations, the controller is constructed with three continuous terms including an integral term that acts as an adaptive controller. The proposed controller is able to accomplish a non-overshoot transient response, a short settling time, and strong disturbance rejection performance for robotic manipulators. The developed model-free control method is implemented on the PUMA 560 robotic manipulator, and its performance is compared with the proportional-derivative (PD) plus gravity controller. Numerical results under measurement noise and load disturbances are provided in order to show the efficacy, validity, and feasibility of the method.

This is an open access article under the [CC BY-SA](https://creativecommons.org/licenses/by-sa/4.0/) license.



Corresponding Author:

Günyaz Ablay

Department of Electrical-Electronics Engineering, Abdullah Gül University

Kayseri, Türkiye

Email: gunyaz.ablay@agu.edu.tr

1. INTRODUCTION

The main issues in robot control problems include accurate reference tracking, load disturbance rejection and robustness to parameter variations. When all these relatively important requirements are taken into account, the high-precision robot control problem presents some challenges due to the coupled nonlinear dynamics of robotic systems. Various control schemes that may be divided into model-based and model-free control categories have been designed and implemented for robot manipulators to tackle with these challenges. The model-based controller designs include sliding mode control (SMC) [1], [2], computed torque control [3], robust control [4], adaptive control [5], model predictive control [6] and backstepping control [7]. The model uncertainties stemming from frictions, parametric uncertainties and load disturbances are the inherent issues of the model-based controllers. To eliminate the effects of these uncertainties, robust, adaptive and machine learning techniques have been used in the model-based control designs [8]–[10]. Specifically, many forms of SMC approaches have been designed for robot manipulators including traditional SMC [11], integral SMC [12], fuzzy SMC [13], backstepping SMC [7], [14], terminal SMC [15], [16], second-order SMCs [17], non-singular terminal SMC [18], fast terminal SMC [19], time-delay estimation based SMC [20] and adaptive SMC [21], [22], but these approaches require an accurate robot model to assure a good control response.

In recent years, some model-free control approaches have also been designed for robot manipulators. Since, in general, a model (or model accuracy) is not considered in the control designs, the model-free control methods offer some advantageous alternative approaches for robot control problems. The PD and PD plus gravity controllers are the most common and highly effective model-free or minimum model requiring

controllers for the industrial robotic manipulators [23], [24]. Machine learning-based controllers including neural networks and fuzzy logic approaches are also designed in this context [25]. A data-driven observer-based model-free adaptive discrete-time terminal SMC [26], an extended state observer-based controller [27], the PID control [28], [29] and an intelligent proportional-derivative SMC [30] have also been designed as model-free controllers. The designed model-free controllers mostly consist of a controller plus estimated robot dynamics, i.e., the alternative model-free controllers have virtually the same structure as the PD plus gravity controller, but they have more complicated control design procedures and their control performances are not significantly better than the PD plus gravity controller.

In this study, a model-free integral SMC is proposed for robust control of robot manipulators without any need for the system model. The inherent robustness of SMC can properly cope with the highly coupled non-linear dynamics of robot manipulators. Many SMC forms have been designed for robot manipulators, but these approaches require a robot model to assure a good response or otherwise can exhibit poor tracking performance. In this work, a three-term model-free continuous integral SMC is designed in order to assure high tracking accuracy, fast convergence, and strong robustness against disturbances. The input–output information of the robot without using any model parameters is utilized in the proposed controller design. The numerical results in both joint-space and task-space implementations are provided for the PUMA-560 robotic arm to illustrate the performance of the proposed controller. The results of the method are compared with the industrial PD plus gravity controller. The proposed control method is able to provide a short settling time, non-overshoot response, zero steady-state error, and robustness under the existence of load disturbances and parameter variations.

The study is organized as follows. A model-free integral SMC design for both joint-space and task-space controls is presented in sections 2 and 3, respectively. Section 4 presents an application of the control method to the PUMA 560 robot, and section 5 concludes the paper.

2. JOINT-SPACE ROBOT CONTROL WITH A MODEL-FREE INTEGRAL SMC

The closed-form dynamic equations of an n-DOF robotic manipulator can be given by (1):

$$M(q)\ddot{q} + C(q, \dot{q})\dot{q} + G(q) = \tau \quad (1)$$

where the joint parameters are defined with n-dimensional joint position vector $q(t)$, joint velocity vector $\dot{q}(t)$ and joint acceleration vector $\ddot{q}(t)$. The actuation torques for each joint are given by $\tau \in R^n$. The positive definite and symmetric matrix $M(q) \in R^{n \times n}$ is the inertia matrix, $C(q, \dot{q}) \in R^{n \times n}$ is the Coriolis/centripetal term, and $G(q) \in R^n$ is the vector of gravitational forces. The inertia matrix is bounded with $m_l I \leq M(q) \leq m_u I$ where m_l and m_u denote positive constants and I is the identity matrix. The robotic manipulators satisfy the skew-symmetric relationship, i.e.,

$$q^T (\dot{M}(q) - 2C(q, \dot{q}))q = 0 \quad (2)$$

For all $q \in R^n$, the Coriolis/centripetal term is bounded by a quadratic function as (3):

$$\|C(q, \dot{q})\dot{q}\| \leq c_0 \|\dot{q}\|^2 \quad (3)$$

where c_0 is a known scalar function (or a positive constant). The gravity vector is also bounded with $\|G(q)\| \leq g_0$ for a finite constant $g_0 > 0$.

The control purpose of the robotic manipulator is trajectory tracking control (or reference regulation as its special case). Designing joint-space controllers with smooth joint-space trajectories is the most common approach. Consider a tracking error vector with a position control objective as (4):

$$\left\{ e = q - q_d : \lim_{t \rightarrow \infty} e = 0 \right\} \quad (4)$$

where q_d is a reference signal vector. The control problem is to find a suitable actuation torque τ such that the position error goes to zero, $e \rightarrow 0$ as $t \rightarrow \infty$. The control system must achieve this control objective with a good transient response to reference changes, and it should reject load disturbances and tackle measurement noise. The common industrial controllers include the PD control or PD plus gravity control methods for providing desired control goals for robot manipulators. Hence, the PD plus gravity controller will first be revisited, then a model-free controller will be introduced, and finally, the results will be provided comparatively.

2.1. Revisiting the industrial PD plus gravity controller

Reference regulation of robotic manipulators is commonly accomplished by independent joint PD control law with a gravity compensation term [23]. It is well-known that a full compensation of gravity vector is not fully possible for degree-of-freedom (n-DoF) rigid manipulators, while the control performance can significantly be improved with the gravity term. The PD plus gravity controller has the form of (5).

$$\tau = -K_p e - K_d \dot{e} + \hat{G}(q) \quad (5)$$

where the control matrices $K_p \in R^{n \times n}$ and $K_d \in R^{n \times n}$ are positive-definite and diagonal matrices and $\hat{G} \in R^n$ is an approximate value of the gravity vector $G(q)$. Substituting (5) into (1), the closed-loop system can be written as (6):

$$M(q)\ddot{q} + C(q, \dot{q})\dot{q} + \tilde{G}(q) + K_d \dot{e} + K_p e = 0 \quad (6)$$

where $\tilde{G} = G - \hat{G}$. If the reference is a constant, then the PD plus gravity controller is quite effective. For stability analysis, consider a positive-definite Lyapunov function as (7):

$$V = \frac{1}{2} \dot{q}^T M(q) \dot{q} + \frac{1}{2} e^T K_p e \quad (7)$$

The time-derivative of (7) is negative definite for a constant reference signal $\dot{q}_d = 0$ and the skew-symmetric robot property $\dot{q}^T (\dot{M} - 2C) \dot{q} = 0$, namely,

$$\dot{V} \leq -\lambda_{\min}(K_d) \|\dot{q}\|^2 + \|\tilde{G}\| \|\dot{q}\| \quad (8)$$

where λ_{\min} is the smallest diagonal element of K_d . Thus, the stability is assured with $\dot{V} \leq 0$ if $\lambda_{\min}(K_d) \|\dot{q}\| \geq \|\tilde{G}\|$. The steady-state error approaches to zero, but not becoming zero because the equilibrium point of the closed loop system *ref6* is found as (9):

$$\tilde{G}(q_e) + K_p e_e = 0 \Rightarrow e_e = -\tilde{G}(q_e)/K_p \quad (9)$$

where q_e and e_e denote equilibrium points. Since $\|\tilde{G}\| \leq \tilde{g}_0$ for a constant $\tilde{g}_0 > 0$, the error is bounded. In addition, in practical implementations, the term $\hat{G}(q)$ is replaced with $\hat{G}(q_d)$ (known as PD plus desired gravity compensation), where q_d is the reference signal. Therefore, the PD plus gravity controller requires large proportional control gains to drive the error to the close vicinity of zero, which might excite measurement noise and high-frequency system dynamics [23].

2.2. A model-free integral SMC design

The SMC provides robust control solutions, but the reaching and sliding phases may require a long time and high control effort due to the conservative bounds of the model uncertainty. To ensure high control performance, fast convergence, and robustness against disturbances and robot manipulator variations, a three-term model-free integral SMC can be defined by (10):

$$\begin{aligned} \tau &= -K_0 s - K_1 |s|^\alpha \operatorname{sgn}(s) - \tau_0 \\ \dot{\tau}_0 &= K_2 |s|^\alpha \operatorname{sgn}(s) \\ s &= \dot{e} + K e \end{aligned} \quad (10)$$

where tracking error e is defined as $e = q - q_d$ for a reference signal q_d , control gain matrices are defined with positive diagonal components as $K_0 = \operatorname{diag}\{k_{01}, \dots, k_{0n}\}$, $K_1 = \operatorname{diag}\{k_{11}, \dots, k_{1n}\}$, $K_2 = \operatorname{diag}\{k_{21}, \dots, k_{2n}\} > 0$, $K = \operatorname{diag}\{k_1, \dots, k_n\} > 0$, and $0 \leq \alpha \leq 1$. The function, $|s|^\alpha \operatorname{sgn}(s)$, is defined in the component-wise form as (11):

$$|s|^\alpha \operatorname{sgn}(s) = [|s_1|^\alpha \operatorname{sgn}(s_1), \dots, |s_n|^\alpha \operatorname{sgn}(s_n)]^T \quad (11)$$

where $\operatorname{sgn}(s_i) = s_i/|s_i|$. To facilitate the operations, a virtual reference vector \dot{q}_r is defined as (12):

$$\dot{q}_r = \dot{q} - s \quad (12)$$

Substituting the control law (10) into the robot equation (1), the closed-loop system dynamics are obtained as (13):

$$M\dot{s} = \tau - M\ddot{q}_r - C\dot{q}_r - G(q) - Cs \quad (13)$$

Consider a positive definite Lyapunov function for stability analysis of the closed-loop system as (14):

$$V = \frac{1}{2}s^T M(q)s \quad (14)$$

The time-derivative of (14) can be written as (15):

$$\begin{aligned} \dot{V} &= s^T M\dot{s} + \frac{1}{2}s^T \dot{M}s \\ &= s^T [\tau - M\ddot{q}_r - C\dot{q}_r - G] - s^T Cs + \frac{1}{2}s^T \dot{M}s \\ &= -s^T K_0 s - s^T \Delta - \sum_{i=1}^n k_{1i} |s_i|^{\alpha+1} \\ &\leq -\sum_{i=1}^n [k_{0i} |s_i| + k_{1i} |s_i|^\alpha - |\Delta_i|] |s_i| \end{aligned} \quad (15)$$

where $s^T (\dot{M} - 2C)s = 0$ due to the skew-symmetric property, and $\Delta = M\ddot{q}_r + C\dot{q}_r + G + \tau_0$. The stability is achieved with $\dot{V} \leq 0$ if $(k_{0i} |s_i| + k_{1i} |s_i|^\alpha) \geq |\Delta_i|$. For $\alpha = 0.5$, a solution of this condition yields (16):

$$|s_i| \geq \frac{1}{2k_{0i}^2} [k_{1i}^2 + 2k_{0i}d_0 - k_{1i}(k_{1i}^2 + 4k_{0i}d_0)^{1/2}] \quad (16)$$

where $|\Delta_i| \leq d_0$. Thus, the control signal drives the robot states into the bounded set (16) in finite time. Since $\dot{V} \leq 0$, the system is stable, and the trajectory reaches the sliding surface in finite time and stays in a very close neighborhood of it. The bounded set can be designed to be very small with large control gain choices, i.e., the robustness and practical stability of the controller are assured when $k_{1i} > d_0$ and $k_{0i} > 0$. Once the robot trajectory reaches this bounded set, then all the state variables will virtually have their steady-state values. For a constant reference signal q_d , a unique steady-state solution of the closed-loop system (13) is found by setting all derivatives to zero as (17):

$$G(q_e) = -K_2 \int_0^\infty |s_e|^\alpha \text{sgn}(s_e) dt \quad (17)$$

where q_e and s_e denote equilibrium points. This implies that the term Δ in (15) will approach zero, $d_0 \rightarrow 0$ with $t \rightarrow \infty$, and thus, the bounded set (16) will go to zero $|s_i| \rightarrow 0$. Due to the fact that the differentiable function $V(t)$ has a finite limit as $t \rightarrow \infty$, and $\dot{V}(t)$ is uniformly continuous, $V(t) \rightarrow 0$ as $t \rightarrow \infty$ according to Barbalat's lemma [31]. This means that the error functions e and \dot{e} tend to zero as time goes to infinity.

There are five control parameters to be determined. The features of these control parameters are as follows. The positive diagonal control gain matrices K_0 and K_1 must be selected large enough to guarantee system stability. The integral term of the controller acts as an adaptive controller as seen in equation (17), and is used to compensate for the static system parameters and disturbances. Hence, the disturbance compensation speed of the controller is determined from the value of the gain matrix K_2 , which can be selected as $k_{2i} \geq g_0$ (upper bound of gravity vector). The control parameters K determine the speed of the transient response of the control system. The parameter α is selected as $\alpha = 0.5$ for good robustness and noise rejection features. Finally, the controller may encounter the chattering phenomenon, so the discontinuous switching function, $\text{sgn}(\cdot)$, may be replaced with its smooth approximates (e.g., sigmoidal or saturation functions) in practical applications with guaranteed uniform ultimate boundedness of errors.

2.3. Task-space robot control with model-free integral SMC

The joint-space control method describes robot movements using the torque and angular positions and velocities that are necessary to complete the task. While the joint-space control is designed by default, it needs

inverse kinematics to calculate the desired joint-space reference trajectories for completing a task, which possesses some difficulties. An alternative approach is the task-space (or Cartesian-space) control, in which the forward kinematics and Jacobian matrix calculations are used to transform between joint-space variables (q_1, \dots, q_n) to task-space variables (x_1, \dots, x_m) . The task-space control is commonly designed with the inverse Jacobian or transpose Jacobian regulators to deal with a mechanical impedance of the robot end effector [32], [33]. The advantage of the task-space control approach is to operate directly on the task-space variables, but the effects of singularities and redundancy cannot easily be managed, and it may become computationally demanding if velocities and accelerations are of concern [34].

The forward kinematics is used to find the pose of the end-effector. Given the joint angles $q \in R^n$, the end-effector pose $x \in R^m$ is defined by (18).

$$x = f(q), f : R^n \rightarrow R^m \quad (18)$$

The differential relationship between the joint displacements and the resulting end-effector motion is represented by the Jacobian matrix as (19):

$$\dot{x} = J(q)\dot{q}, J(q) = \partial f(q)/\partial q \quad (19)$$

where $J(q) \in R^{m \times n}$ is the analytical Jacobian matrix standing for the mapping from joint space to task space. The transpose of the Jacobian is also used to describe the torque and force relations by (20),

$$\tau = J(q)^T F \quad (20)$$

where $F \in R^m$ is the applied force at the end-effector in task space. The Jacobian transpose method eliminates the issues related to the Jacobian inversion and singularity problems, and thus it is used to obtain the robot model in the task space as (21),

$$M(x)\ddot{x} + C(x, \dot{x})\dot{x} + G(x) = F \quad (21)$$

where $M(x) = J^{-T}M(q)J^{-1}$, $C(x, \dot{x}) = J^{-T}C(q, \dot{q})J^{-1} - J^{-T}M(q)J^{-1}\dot{J}J^{-1}$ and $G(x) = J^{-T}G(q)$.

It is assumed that the Jacobian matrix is nonsingular, but if it is singular then the system has redundancy for the given task in the task space. The task-space robot equation has the similar properties to joint-space robot equation, including the skew-symmetric property $\dot{x}^T(\dot{M} - 2C)\dot{x} = 0$ and boundedness of the other robot equation terms [35]. Therefore, the joint-space controllers can also be designed in a similar form for the task-space representations.

In task space a tracking error vector with a position control objective is defined as (22):

$$\left\{ e = x - x_d : \lim_{t \rightarrow \infty} e = 0 \right\} \quad (22)$$

where x_d is a reference signal vector. To achieve this tracking control goal for (21), similar to (10) a model-free integral SMC can be defined as (23):

$$\begin{aligned} F &= -K_0 s - K_1 |s|^\alpha \operatorname{sgn}(s) - f_0 \\ \dot{f}_0 &= K_2 |s|^\alpha \operatorname{sgn}(s) \\ s &= \dot{e} + K e \end{aligned} \quad (23)$$

where $e = x - x_d$ for a reference signal x_d . Similar to the joint-space controller analysis, for a Lyapunov function, $V = 0.5s^T M(x)s$, we can show that its time-derivative is negative definite as $\dot{V} \leq 0$ under the controller (23). Namely, the error functions e and \dot{e} tend to zero as time goes to infinity.

The general task-space control and joint-space control schemes are illustrated in Figure 1. There are different pros and cons to trajectory planning and control in joint space or task space. For example, joint-space trajectories have smooth actuator motion and have no problem with singularities, while inverse kinematics are needed to generate joint-space references. On the other hand, task-space trajectories are easier to visualize and the motion in task-space is more predictable, but it is prone to singularities and the actuator motion is more difficult to verify.

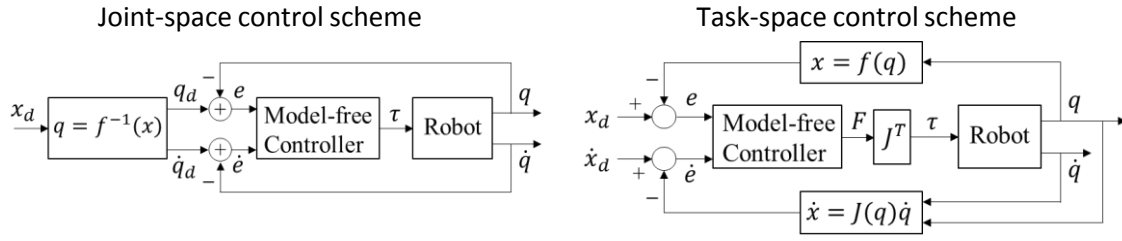


Figure 1. Model-free control implementations in joint-space and task-space of robotic manipulators

3. CONTROL IMPLEMENTATIONS TO PUMA 560 ROBOT

The explicit dynamic model of the PUMA 560 robot is given by [36]:

$$M(q)\ddot{q} + B(q)\dot{q}_i\dot{q}_j + C(q, \dot{q})\dot{q}_i^2 + G(q) = \tau - \tau_l \quad (24)$$

where τ_l is the load torque, $B(q)$ is the matrix of Coriolis forces, $C(q)$ is the matrix of Centrifugal forces, and $i \neq j$ for $i, j = 1, \dots, 6$. The PUMA 560 robot matrix/vectors can be defined by $M = [m_{ij}]$, $B = [b_{ijk}]$, $C = [c_{ij}]$, $G = [G_i]$, whose components are given by [36],

$$m_{11} = I_m 1 + I_1 + I_3 C C_2 + (I_7 + I_{21} + 2I_{15}) S S_{23} + (I_{10} + 2I_{22}) S C_{23} + I_{11} S C_2 + 2C_2 [I_5 S_{23} + I_{12} C_{23} + I_{16} S_{23}]$$

$$m_{12} = I_4 S_2 + I_8 C_{23} + I_9 C_2 + I_{13} S_{23} - I_{18} C_{23}$$

$$m_{13} = I_8 C_{23} + I_{13} S_{23} - I_{18} C_{23}$$

$$m_{22} = I_m 2 + I_2 + I_6 + 2[I_5 S_3 + I_{12} C_2 + I_{15} + I_{16} S_3]$$

$$m_{23} = I_5 S_3 + I_6 + I_{12} C_3 + I_{16} S_3 + 2I_{15}$$

$$m_{33} = I_m 3 + I_6 + 2I_{15}$$

$$m_{35} = I_{15} + I_{17}$$

$$m_{44} = I_m 4 + I_{14}$$

$$m_{55} = I_m 5 + I_{17}$$

$$m_{66} = I_m 6 + I_{23}$$

$$m_{21} = m_{12}, m_{31} = m_{13}, m_{32} = m_{23}$$

$$b_{112} = 2[-I_3 S C_2 + (I_5 + I_{16}) C_{223} + (I_7 + 2I_{15} + I_{21}) S C_{23} - I_{12} S_{223}] + (I_{10} + 2I_{22})(1 - 2S S_{23}) + I_{11}(1 - 2S S_2)$$

$$b_{113} = 2[(I_5 + I_{16}) C_2 C_{23} + (I_7 + 2I_{15} + I_{21}) S C_{23} - I_{12} C_2 S_{23} + I_{22}(1 - 2S S_{23})] + I_{10}(1 - 2S S_{23})$$

$$b_{115} = 2[-S C_{23} + I_{15} S C_{23} + I_{16} C_2 C_{23} + I_{22} C C_{23}]$$

$$b_{123} = 2[-I_8 S_{23} + I_{13} C_{23} + I_{18} S_{23}]$$

$$b_{214} = I_{14} S_{23} + I_{19} S_{23} + I_{20} S_{23}$$

$$b_{223} = 2[-I_{12} S_3 + I_5 C_3 + I_{16} C_3]$$

$$b_{225} = 2[I_{16} C_3 + I_{22}]$$

$$b_{235} = 2[I_{16} C_3 + I_{22}]$$

$$b_{314} = I_{20} S_{23} + I_{14} S_{23} + I_{19} S_{23}$$

$$b_{412} = -b_{214}$$

$$b_{413} = -b_{314}$$

$$b_{415} = -I_{20} S_{23} - I_{17} S_{23}$$

$$b_{514} = -b_{415}$$

$$c_{12} = I_4 C_2 - I_8 S_{23} - I_9 S_2 + I_{13} C_{23} + I_{18} S_{23}$$

$$c_{13} = 0.5b_{123}$$

$$c_{21} = -0.5b_{112}$$

$$c_{23} = 0.5b_{223}$$

$$c_{31} = -0.5b_{113}$$

$$c_{32} = -c_{23}$$

$$c_{51} = -0.5b_{115}$$

$$c_{52} = -0.5b_{225}$$

$$G_2 = g_1 C_2 + g_2 S_{23} + g_3 S_2 + g_4 C_{23} + g_5 S_{23}$$

$$G_3 = g_2 S_{23} + g_4 C_{23} + g_5 S_{23}$$

$$G_5 = g_5 S_{23}$$

where $S_i = \sin(q_i)$, $C_i = \cos(q_i)$, $C_{ij} = \cos(q_i + q_j)$, $S_{ijk} = \sin(q_i + q_j + q_k)$, $CC_i = \cos(q_i)^2$ and $CS_i = \cos(q_i) \sin(q_i)$, and all other elements of the matrices are zero. The PUMA 560 robot arm constants and DH parameter values are provided in Tables 1 and 2, respectively.

Table 1. Inertial (kg/m^2) and gravitational (Nm) constants

No	Inertial (kg/m^2)	Gravitational (Nm) constants	No	Inertial (kg/m^2)	Gravitational (Nm) constants
1	I_1	1.43	18	I_{18}	0.000431
2	I_2	1.75	19	I_{19}	0.0003
3	I_3	1.38	20	I_{20}	-0.000202
4	I_4	0.69	21	I_{21}	-0.0001
5	I_5	0.372	22	I_{22}	-0.000058
6	I_6	333	23	I_{23}	0.00004
7	I_7	298	24	I_{m1}	1.14
8	I_8	-0.134	25	I_{m2}	4.71
9	I_9	0.0238	26	I_{m3}	0.827
10	I_{10}	-0.0213	27	I_{m4}	0.2
11	I_{11}	-0.0142	28	I_{m5}	0.179
12	I_{12}	-0.011	29	I_{m6}	0.193
13	I_{13}	-0.00379	30	g_1	-37.2
14	I_{14}	0.00164	31	g_2	-8.44
15	I_{15}	0.00125	32	g_3	1.02
16	I_{16}	0.00124	33	g_4	0.249
17	I_{17}	0.000642	34	g_5	-0.0282

Table 2. PUMA 560 arm DH parameters

Link i	q_i	α_i	a_i	d_i
1	q_1	-90	0	0
2	q_2	0	0.4318	0.14909
3	q_3	90	0.0203	0
4	q_4	-90	0	0.43307

The PUMA 560 robotic arm has six axes, but the last three axes form only a spherical wrist as seen in Figure 2. The control results are provided when the last three axes (q_4, q_5, q_6) of the robotic arm are locked, and thus results corresponding to the first three axes (q_1, q_2, q_3) are provided. The torque constraints of the PUMA 560 robot are taken into consideration in joint-space and task-space control designs, which are given by $|\tau_1| \leq 97.6$, $|\tau_2| \leq 186.4$, $|\tau_3| \leq 89.4$, $|\tau_4| \leq 24.2$, $|\tau_5| \leq 20.1$ and $|\tau_6| \leq 21.3$ Nm. In numerical studies, the contributions from measurement noise and load disturbances are considered. It is assumed that the angular position and angular velocity measurements are exposed to normally distributed measurement noise with a mean of $\mu = 0$ and a standard deviation of $\sigma(q) = 0.172$ deg (or ± 0.5 deg in magnitude) and $\sigma(\dot{q}) = 0.5$ deg/s (or ± 1.43 deg/s in magnitude). Step load disturbances with $\tau_i = 10$ Nm magnitude (around 10% of the first three joint torque limits) are added to system torque inputs at $t = 5$ s for evaluating load disturbance rejection performances of the controllers.

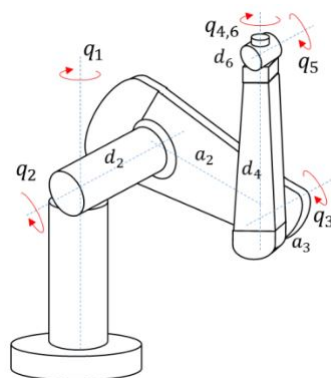


Figure 2. Schematic diagram of the PUMA 560 robotic manipulator

3.1. Joint-space control results

Joint-space control results are provided in Figure 3 to Figure 8 for both PD plus gravity and the proposed model-free integral SMC controllers. The control gains are selected such that controllers provide non-overshoot responses and take into account the torque constraints of the PUMA 560 robotic manipulator. The PD plus gravity controller gain matrices are taken as $K_p = 500 I_3$ and $K_d = 100 I_3$ where $I_3 \in R^{3 \times 3}$ is the identity matrix. The model-free integral SMC controller gain matrices are chosen as $K_0 = 60 I_3$, $K_1 = 50 I_3$, $K_2 = 200 I_3$, $K = 5 I_3$ and $\alpha = 0.5$. It should be noted that the discontinuous function of the controller is approximated as $sgn(s_i) \approx sat(s_i/5)$ in the implementations to avoid possible chattering in the torque control inputs. The control parameters are selected such that both controllers can have very close performances for comparison targets.

Performances of the controllers for constant references, $q_d = (\pi/4, \pi/2, -\pi/4)$, are illustrated in Figures 3 to 5. Figure 3 shows that both controllers have non-overshoot transient responses and reach the steady-state conditions in less than 0.5 s with zero steady-state error under no-load conditions. Figure 4 shows the torque control signals of the controllers, in which both controllers produce almost the same torque inputs. Load disturbance rejection performances of the controllers are assessed for a step load $\tau_l = 10$ Nm (less than 10% of the joint torque limits) added to system torque inputs at $t = 5$ s as seen in Figure 4. Under the load disturbance, Figure 5 shows that the model-free integral SMC controller quickly eliminates the effects of the load disturbance and provides zero steady-state errors. However, the PD plus gravity controller provides an erroneous performance under load disturbance. Hence, the proposed model-free integral SMC controller provides robustness to the robotic manipulator control against load disturbances.

Figure 6 shows the disturbance estimation performance of the controller. The integral term τ_0 of the controller acts as an adaptive controller and compensates for the static system terms and disturbances. Under no-load conditions, it is seen in the figure that the integral control components approach to the gravity components, $\tau_{01} \rightarrow G_1$, $\tau_{02} \rightarrow G_2$, and $\tau_{03} \rightarrow G_3$. When a step load $\tau_l = 10$ Nm is added to system torque inputs at $t = 5$ s, the integral control components approach to the total values of static terms, i.e., $\tau_{01} \rightarrow G_1 + \tau_{l1}$, $\tau_{02} \rightarrow G_2 + \tau_{l2}$, and $\tau_{03} \rightarrow G_3 + \tau_{l3}$. The gain matrix K_2 determines the disturbance compensation speed of the controller, i.e., the larger the gain, the faster convergence is observed, but an oscillation in the robot trajectory can be seen with large integral control gain values. Hence, there is a trade-off between controller performance and disturbance rejection response speed.

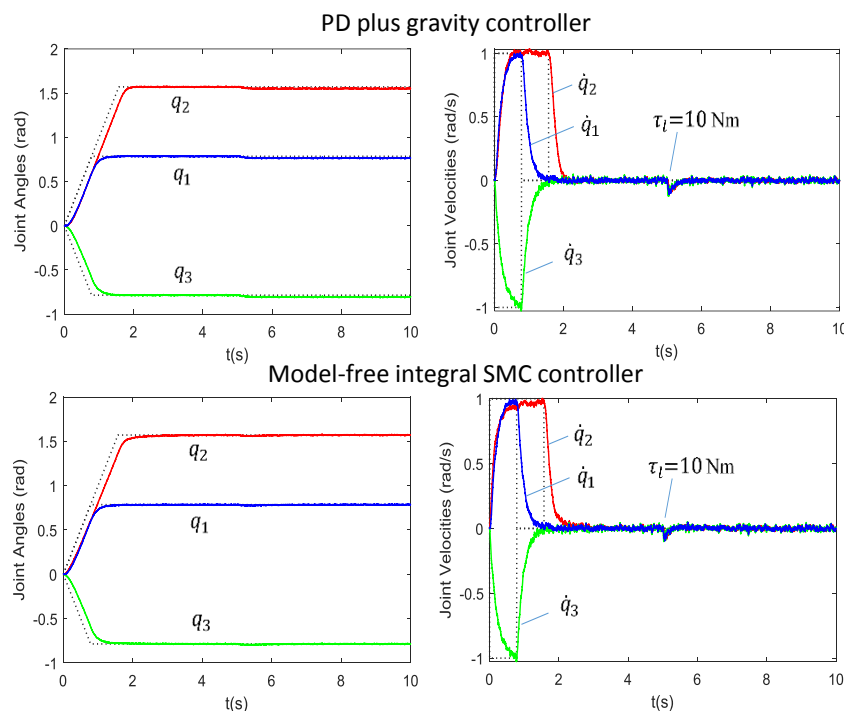


Figure 3. Constant reference tracking control performances for joint positions and velocities under $\tau_l = 10$ Nm load torque

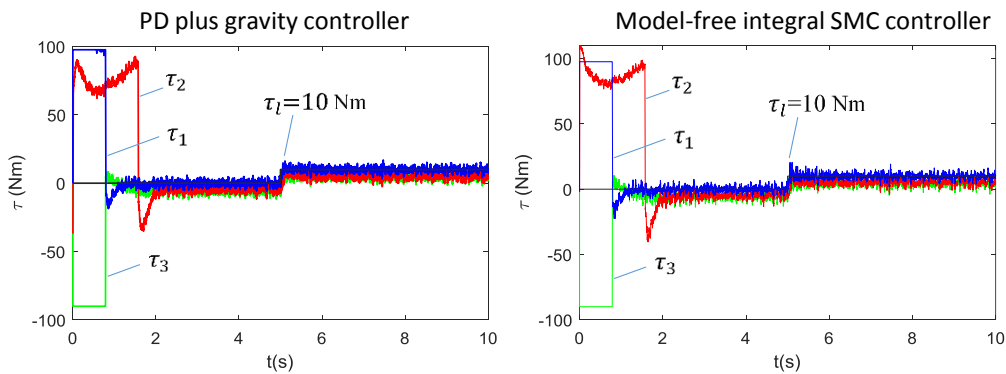


Figure 4. Control torque signals for each joint for constant references

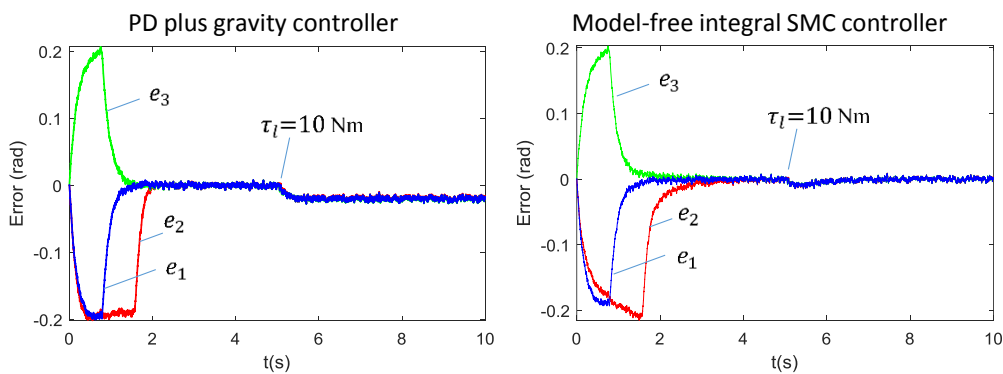


Figure 5. Constant reference tracking errors under $\tau_l = 10$ Nm load torques

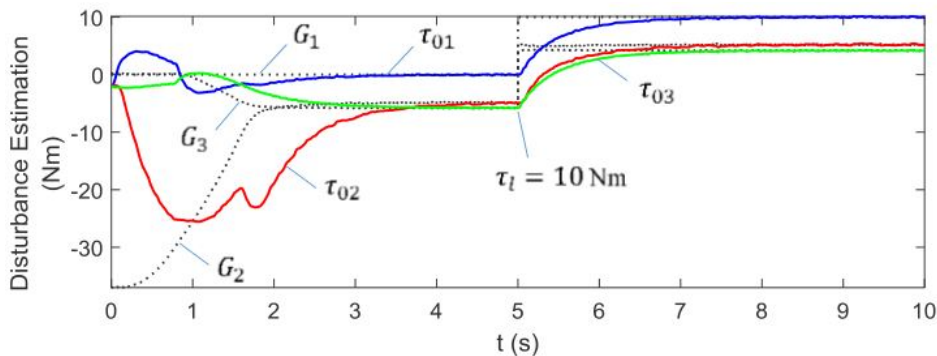


Figure 6. Disturbance estimation with an integral term of the model-free integral SMC controller

Figures 7 to 9 show the performances of the controllers for sinusoidal reference signals. Figure 7 displays non-overshoot transient responses and less than 0.5 s settling time with zero steady-state error in joint positions and velocities for both controllers under no-load disturbances. When a step load $\tau_l = 10$ Nm is added to system torque inputs at $t = 5$ s as seen in Figure 8, the PD plus gravity controller provides a constant steady-state error. On the other hand, the proposed model-free integral SMC controller quickly recovers the effects of load disturbances. The load disturbance rejection performances of the controllers can easily be seen in Figure 9. The phase-plane portraits (x vs y) are plotted when a step load $\tau_l = 10$ Nm is added to system torque inputs at $t = 0$ s as seen in Figure 9. It is clear that there is an offset error for the PD plus gravity controller. Similar to the constant reference case, the model-free integral SMC controller rejects the load disturbance and provides zero steady-state error and robustness to the robotic manipulator.

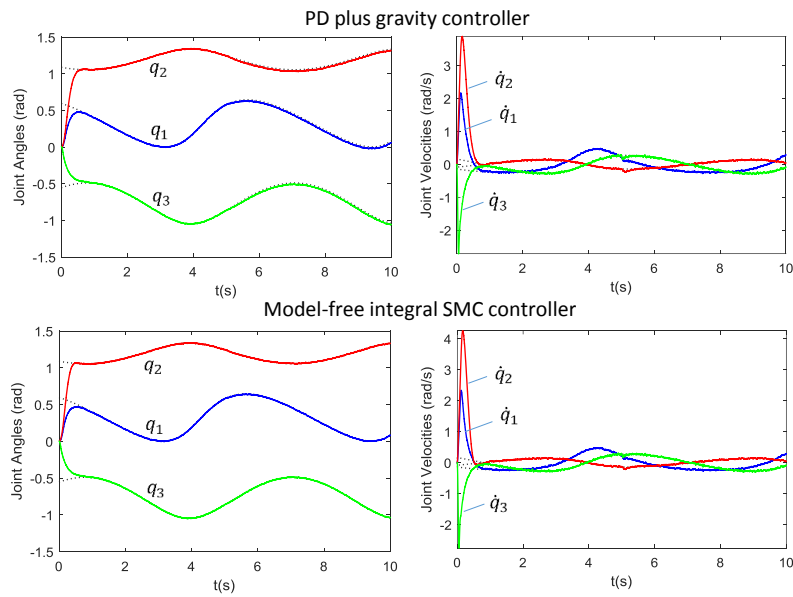


Figure 7. Sinusoidal reference tracking control performances for joint positions and velocities under $\tau_l = 10$ Nm load torque

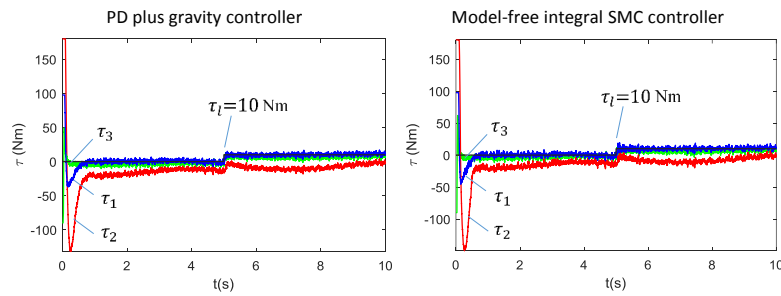


Figure 8. Control torque signals for each joint for sinusoidal references

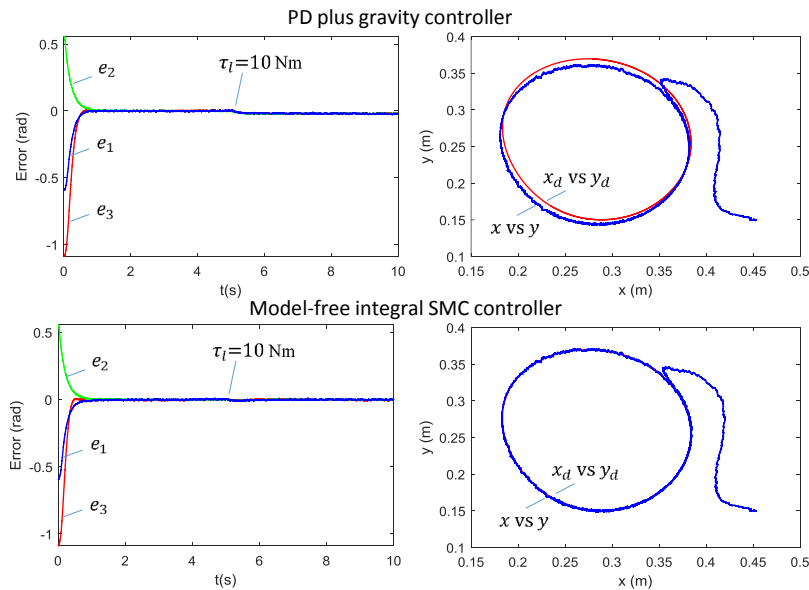


Figure 9. Sinusoidal reference tracking errors under $\tau_l = 10$ Nm load torques

3.2. Task-space control results

For task-space control design, the forward kinematics and its Jacobian matrix are needed as seen in Figure 1. Forward kinematics of the PUMA 560 robot obtained from the DH parameters given in Table 2 when the last three axes (q_4, q_5, q_6) are locked is given by (25):

$$\begin{aligned} x &= C_1(a_2C_2 + a_3C_{23} + d_4S_{23}) - d_2S_1 \\ y &= S_1(a_2C_2 + a_3C_{23} + d_4S_{23}) + d_2C_1 \\ z &= a_2S_2 + a_3S_{23} - d_4C_{23} \end{aligned} \quad (25)$$

where S_1 is used for $\sin(q_1)$, C_1 is used for $\cos(q_1)$, S_{23} is used for $\sin(q_2+q_3)$, and C_{23} is used for $\cos(q_2+q_3)$. The robot parameters are $d_2 = 0.1491$, $d_4 = 0.4331$, $a_2 = 0.4318$ and $a_3 = 0.0203$. The Jacobian matrix of the robot is obtained as $J = [j_{ij}] \in R^{3 \times 3}$ with (26).

$$\begin{aligned} j_{11} &= -S_1(a_2C_2 + a_3C_{23} + d_4S_{23}) - d_2C_1 \\ j_{12} &= C_1(-a_2S_2 - a_3S_{23} + d_4C_{23}) \\ j_{13} &= C_1(-a_3S_{23} + d_4C_{23}) \\ j_{21} &= C_1(a_2C_2 + a_3C_{23} + d_4S_{23}) - d_2S_1 \\ j_{22} &= S_1(-a_2S_2 - a_3S_{23} + d_4C_{23}) \\ j_{23} &= S_1(-a_3S_{23} + d_4C_{23}) \\ j_{31} &= 0, \quad j_{32} = d_4S_{23} + a_3C_{23} + a_2C_2 \\ j_{33} &= d_4S_{23} + a_3C_{23} \end{aligned} \quad (26)$$

Task-space control results for the PUMA 560 robotic manipulator are shown in Figures 10 to 12 for both PD plus gravity and the proposed model-free ISMC controllers. The PD plus gravity controller gain matrices are taken as $K_p = 5000I_3$ and $K_d = 1000I_3$ where $I_3 \in R^{3 \times 3}$ is the identity matrix. The model-free ISMC controller gain matrices are chosen as $K_0 = 600I_3$, $K_1 = 500I_3$, $K_2 = 2000I_3$, $K = 5I_3$ and $\alpha = 0.5$. To eliminate possible chattering in the torque control inputs, the signum function is approximated as $sgn(s_i) \approx sat(s_i/5)$ in the control implementations. Again, as in joint-space control designs, the control parameters are selected such that both controllers can have very close performances for comparison goals. In addition, non-overshoot responses for both controllers are targeted.

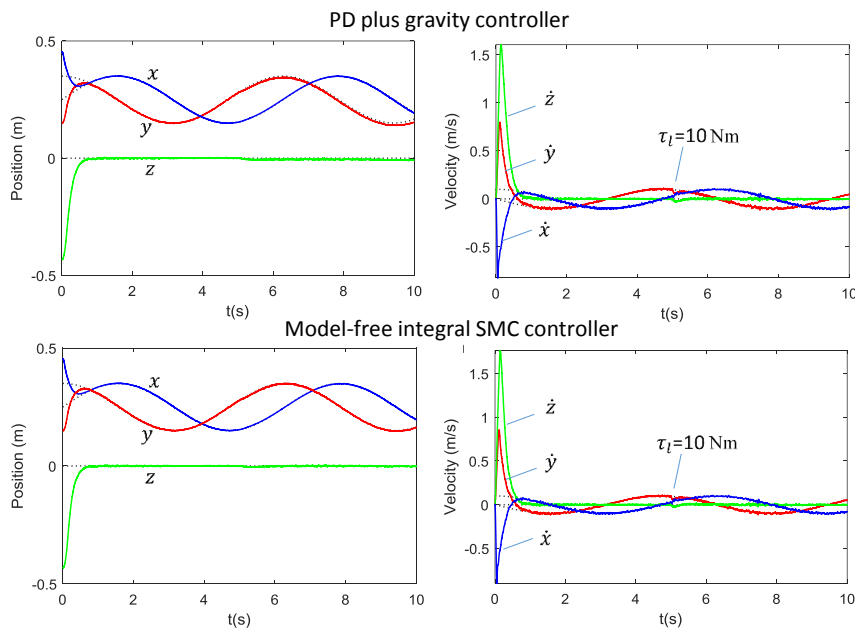


Figure 10. Task-space tracking control performances for joint positions and velocities under $\tau_l = 10$ Nm load torque

Task-space references are taken as $x_d(t) = 0.25 + 0.1 \sin(t)$, $y_d(t) = 0.25 + 0.1 \cos(t)$ and $z_d(t) = 0$. Figure 10 displays task-space tracking control performances for joint positions and velocities under $\tau_l = 10$ Nm load torque applied at $t = 5$ s. It is obvious that both controllers have non-overshoot transient responses and reach the steady-state conditions in less than 0.5 s for both position and velocity reference signals. Figure 11 shows that both controllers produce almost the same torque control signals. Under the load torque disturbances, Figure 12 clearly shows that the model-free integral SMC controller quickly rejects the load disturbance effects and provides a zero steady-state error. However, the PD plus gravity controller is not able to eliminate the load disturbance completely. Similar to the joint space control application results, the proposed model-free integral SMC controller provides robust and highly satisfactory trajectory tracking performance in task-space control of the PUMA 560 robotic arm.

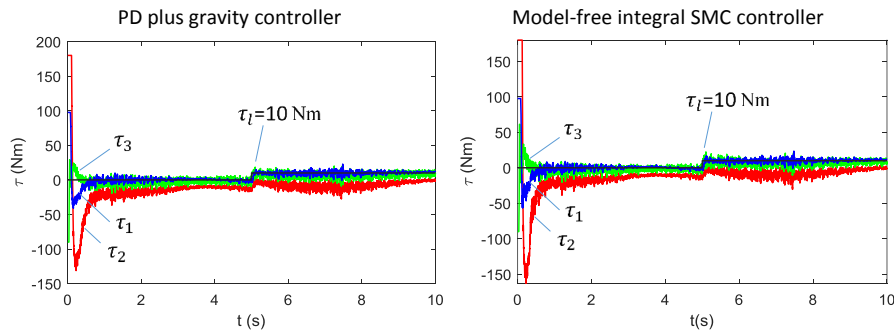


Figure 11. Task-space control torque signals for each joint

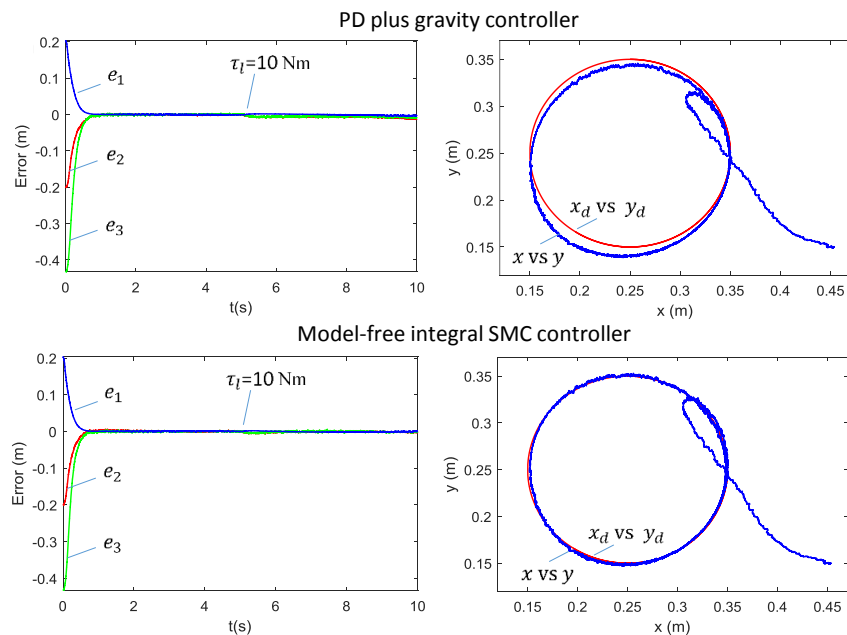


Figure 12. Task-space tracking errors under $\tau_l = 10$ Nm load torques

4. CONCLUSION

A model-free continuous integral sliding mode control approach is proposed for controlling robotic manipulators for providing robust and high control performances. The integral term of the controller has the working principle of adaptive control and dynamically eliminates the effects of static terms such as gravity terms and load disturbances. The controller is completely model-free and utilizes the robustness feature of the sliding mode control for the global stabilization of robotic manipulators. The proposed controller is designed

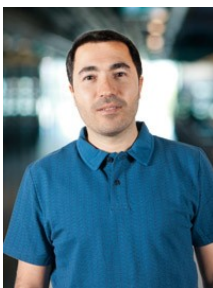
for both joint-space control and task-space control implementations. The performance of the controller is illustrated on the PUMA 560 robotic manipulator and compared with the performance of the PD plus gravity control approach. The numerical results show that the model-free control method is capable of providing a non-overshoot response, fast settling time, zero steady-state error under load disturbance and measurement noise, and is robust under bounded uncertainties.




REFERENCES

- [1] H. Sai, Z. Xu, S. He, E. Zhang, and L. Zhu, "Adaptive nonsingular fixed-time sliding mode control for uncertain robotic manipulators under actuator saturation," *ISA Transactions*, vol. 123, pp. 46–60, Apr. 2022, doi: 10.1016/j.isatra.2021.05.011.
- [2] X. Yin, L. Pan, and S. Cai, "Robust adaptive fuzzy sliding mode trajectory tracking control for serial robotic manipulators," *Robotics and Computer-Integrated Manufacturing*, vol. 72, Dec. 2021, doi: 10.1016/j.rcim.2019.101884.
- [3] J. H. Kim and S. M. Hur, "Induced norm-based analysis for computed torque control of robot systems," *IEEE Access*, vol. 8, pp. 126228–126238, 2020, doi: 10.1109/ACCESS.2020.3007949.
- [4] L. Bascetta and P. Rocco, "Revising the robust-control design for rigid robot manipulators," *IEEE Transactions on Robotics*, vol. 26, no. 1, pp. 180–187, Feb. 2010, doi: 10.1109/TRO.2009.2033957.
- [5] Y. Gao, M. Joo Er, and S. Yang, "Adaptive control of robot manipulators using fuzzy neural networks," *IEEE Transactions on Industrial Electronics*, vol. 48, no. 6, pp. 1274–1278, Dec. 2001, doi: 10.1109/41.969410.
- [6] G. P. Incremona, A. Ferrara, and L. Magni, "MPC for robot manipulators with integral sliding modes generation," *IEEE/ASME Transactions on Mechatronics*, vol. 22, no. 3, pp. 1299–1307, Jun. 2017, doi: 10.1109/TMECH.2017.2674701.
- [7] T. N. Truong, A. T. Vo, and H. J. Kang, "A backstepping global fast terminal sliding mode control for trajectory tracking control of industrial robotic manipulators," *IEEE Access*, vol. 9, pp. 31921–31931, 2021, doi: 10.1109/ACCESS.2021.3060115.
- [8] B. Zhou, L. Yang, C. Wang, G. Lai, and Y. Chen, "Adaptive finite-time tracking control of robot manipulators with multiple uncertainties based on a low-cost neural approximator," *Journal of the Franklin Institute*, vol. 359, no. 10, pp. 4938–4958, May 2022, doi: 10.1016/j.jfranklin.2022.04.025.
- [9] Y. W. Liang, S. D. Xu, D. C. Liaw, and C. C. Chen, "A study of T-S model-based SMC scheme with application to robot control," *IEEE Transactions on Industrial Electronics*, vol. 55, no. 11, pp. 3964–3971, Nov. 2008, doi: 10.1109/TIE.2008.2005138.
- [10] B. M. Yilmaz, E. Tatlicioglu, A. Savran, and M. Alci, "Adaptive fuzzy logic with self-tuned membership functions based repetitive learning control of robotic manipulators," *Applied Soft Computing*, vol. 104, Jun. 2021, doi: 10.1016/j.asoc.2021.107183.
- [11] L. Gracia, F. Garelli, and A. Sala, "Integrated sliding-mode algorithms in robot tracking applications," *Robotics and Computer-Integrated Manufacturing*, vol. 29, no. 1, pp. 53–62, Feb. 2013, doi: 10.1016/j.rcim.2012.07.007.
- [12] S. Nadda and A. Swarup, "Integral sliding mode control for position control of robotic manipulator," in *2018 5th International Conference on Signal Processing and Integrated Networks (SPIN)*, Feb. 2018, pp. 639–642, doi: 10.1109/SPIN.2018.8474267.
- [13] H. Hu and P. Y. Woo, "Fuzzy supervisory sliding-mode and neural-network control for robotic manipulators," *IEEE Transactions on Industrial Electronics*, vol. 53, no. 3, pp. 929–940, Jun. 2006, doi: 10.1109/TIE.2006.874261.
- [14] Y. Wang, Z. Zhang, C. Li, and M. Buss, "Adaptive incremental sliding mode control for a robot manipulator," *Mechatronics*, vol. 82, Apr. 2022, doi: 10.1016/j.mechatronics.2021.102717.
- [15] Z. Ma and G. Sun, "Dual terminal sliding mode control design for rigid robotic manipulator," *Journal of the Franklin Institute*, vol. 355, no. 18, pp. 9127–9149, Dec. 2018, doi: 10.1016/j.jfranklin.2017.01.034.
- [16] Y. Tang, "Terminal sliding mode control for rigid robots," *Automatica*, vol. 34, no. 1, pp. 51–56, Jan. 1998, doi: 10.1016/S0005-1098(97)00174-X.
- [17] J. Zhai and Z. Li, "Fast-exponential sliding mode control of robotic manipulator with super-twisting method," *IEEE Transactions on Circuits and Systems II: Express Briefs*, vol. 69, no. 2, pp. 489–493, Feb. 2022, doi: 10.1109/TC-SII.2021.3081147.
- [18] D. Cruz-Ortiz, I. Chairez, and A. Poznyak, "Non-singular terminal sliding-mode control for a manipulator robot using a barrier Lyapunov function," *ISA Transactions*, vol. 121, pp. 268–283, Feb. 2022, doi: 10.1016/j.isatra.2021.04.001.
- [19] A. Jouila and K. Nouri, "An adaptive robust nonsingular fast terminal sliding mode controller based on wavelet neural network for a 2-DOF robotic arm," *Journal of the Franklin Institute*, vol. 357, no. 18, pp. 13259–13282, Dec. 2020, doi: 10.1016/j.jfranklin.2020.04.038.
- [20] N. Adhikary and C. Mahanta, "Sliding mode control of position commanded robot manipulators," *Control Engineering Practice*, vol. 81, pp. 183–198, Dec. 2018, doi: 10.1016/j.conengprac.2018.09.011.
- [21] M. D. Tran and H. J. Kang, "Adaptive terminal sliding mode control of uncertain robotic manipulators

- based on local approximation of a dynamic system,” *Neurocomputing*, vol. 228, pp. 231–240, Mar. 2017, doi: 10.1016/j.neucom.2016.09.089.
- [22] S. Yi and J. Zhai, “Adaptive second-order fast nonsingular terminal sliding mode control for robotic manipulators,” *ISA Transactions*, vol. 90, pp. 41–51, Jul. 2019, doi: 10.1016/j.isatra.2018.12.046.
- [23] R. Kelly, V. S. Davila, and J. A. L. Perez, *Control of robot manipulators in joint space*. London: Springer, 2005.
- [24] A. Zavala-Río and V. Santibáñez, “A natural saturating extension of the PD-with-desired-gravity-compensation control law for robot manipulators with bounded inputs,” *IEEE Transactions on Robotics*, vol. 23, no. 2, pp. 386–391, Apr. 2007, doi: 10.1109/TRO.2007.892224.
- [25] K. Zheng, Y. Hu, and B. Wu, “Model-free development of control systems for a multi-degree-of-freedom robot,” *Mechatronics*, vol. 53, pp. 262–276, Aug. 2018, doi: 10.1016/j.mechatronics.2018.06.015.
- [26] B. Esmaili, M. Salim, M. Baradarannia, and A. Farzamnia, “Data-driven observer-based model-free adaptive discrete-time terminal sliding mode control of rigid robot manipulators,” in *7th International Conference on Robotics and Mechatronics*, Nov. 2019, pp. 432–438, doi: 10.1109/ICRoM48714.2019.9071819.
- [27] A. Saleki and M. M. Fateh, “Model-free control of electrically driven robot manipulators using an extended state observer,” *Computers and Electrical Engineering*, vol. 87, Oct. 2020, doi: 10.1016/j.compeleceng.2020.106768.
- [28] Y. Su, P. C. Muller, and C. Zheng, “Global asymptotic saturated PID control for robot manipulators,” *IEEE Transactions on Control Systems Technology*, vol. 18, no. 6, pp. 1280–1288, Nov. 2010, doi: 10.1109/TCST.2009.2035924.
- [29] H. Abouaïssa and S. Chouraqui, “On the control of robot manipulator: a model-free approach,” *Journal of Computational Science*, vol. 31, pp. 6–16, Feb. 2019, doi: 10.1016/j.jocs.2018.12.011.
- [30] D. Elleuch, T. Damak, and C. Jiang, “Robust model-free control for robot manipulator under actuator dynamics,” *Mathematical Problems in Engineering*, vol. 2020, Aug. 2020, doi: 10.1155/2020/7417314.
- [31] J. Slotine and W. Li, *Applied nonlinear control*, vol. 199, no. 1. New Jersey: Prentice Hall, 1990.
- [32] H. Sadeghian, L. Villani, M. Keshmiri, and B. Siciliano, “Task-space control of robot manipulators with null-space compliance,” *IEEE Transactions on Robotics*, vol. 30, no. 2, pp. 493–506, Apr. 2014, doi: 10.1109/TRO.2013.2291630.
- [33] D. Nicolis, F. Allevi, and P. Rocco, “Operational space model predictive sliding mode control for redundant manipulators,” *IEEE Transactions on Robotics*, vol. 36, no. 4, pp. 1348–1355, 2020, doi: 10.1109/TRO.2020.2974092.
- [34] X. Li and C. C. Cheah, “Global task-space adaptive control of robot,” *Automatica*, vol. 49, no. 1, pp. 58–69, Jan. 2013, doi: 10.1016/j.automatica.2012.07.003.
- [35] P. Sanchez-Sanchez and F. Reyes-Cortes, “Cartesian control for robot manipulators,” in *Robot Manipulators Trends and Development*, London: InTech, 2010.
- [36] B. Armstrong, O. Khatib, and J. Burdick, “The explicit dynamic model and inertial parameters of the PUMA 560 arm,” in *IEEE International Conference on Robotics and Automation*, 1986, vol. 3, pp. 510–518, doi: 10.1109/ROBOT.1986.1087644.

BIOGRAPHIES OF AUTHORS



Günyaz Ablay    is currently working at Abdullah Gul University. He received his Ph.D. degree in Nuclear Engineering from the Ohio State University, and his M.S. and B.S. degrees in Electrical-Electronics Engineering from Firat University. His research interests include control theory and its applications, embedded control, robotics, nonlinear dynamics, chaos theory, and nuclear energy technologies. He can be contacted at gunyaz.ablay@agu.edu.tr.